Climatic Change
DOI 10.1007/s10584-010-9926-2

Sensitivity of discharge and flood frequency to twenty-first century and late Holocene changes in climate and land use (River Meuse, northwest Europe)

Philip J. Ward · Hans Renssen · Jeroen C. J. H. Aerts · Peter H. Verburg

Received: 28 July 2008 / Accepted: 22 June 2010

Abstract We used a calibrated coupled climate–hydrological model to simulate Meuse discharge over the late Holocene (4000–3000 BP and 1000–2000 AD). We then used this model to simulate discharge in the twenty-first century under SRES emission scenarios A2 and B1, with and without future land use change. Mean discharge and medium-sized high-flow (e.g. Q_{99}) frequency are higher in 1000–2000 AD than in 4000–3000 BP; almost all of this increase can be attributed to the conversion of forest to agriculture. In the twentieth century, mean discharge and the frequency of medium-sized high-flow events are higher than in the nineteenth century; this increase can be attributed to increased (winter half-year) precipitation. Between the twentieth and twenty-first centuries, anthropogenic climate change causes a further increase in discharge and medium-sized high-flow frequency; this increase is of a similar order of magnitude to the changes over the last 4,000 years. The magnitude of extreme flood events (return period 1,250-years) is higher in the twenty-first century than in any preceding period of the time-slices studied. In contrast to the long-term influence of deforestation on mean discharge, changes in forest cover have had little effect on these extreme floods, even on the millennial timescale.

P. J. Ward (✉) · J. C. J. H. Aerts · P. H. Verburg
Institute for Environmental Studies (IVM),
Faculty of Earth and Life Sciences,
VU University Amsterdam, De Boelelaan 1085,
1081 HV Amsterdam, The Netherlands
e-mail: philip.ward@ivm.vu.nl

H. Renssen
Department of Earth Sciences,
Faculty of Earth and Life Sciences,
VU University Amsterdam,
Amsterdam, The Netherlands

Published online: 24 August 2010

1 Introduction

The relatively large number of high-flow events on the River Meuse (Fig. 1) in recent years, compared to the rest of the twentieth century (De Wit et al. 2007a), has led to widespread public, academic, and political interest. Future climate change is expected to have major impacts on river discharge (Kundzewicz et al. 2007), and hence many modelling studies have been carried out to assess the potential changes in Meuse discharge and flood frequency in the twenty-first century (e.g. Booij 2005; Bultot et al. 1988, 1990; De Wit et al. 2001, 2007b; Gellens 1991; Gellens and Roulin 1998; Middelkoop et al. 2004; Van Deursen and Middelkoop 2001, 2002).

To date, these studies have used models calibrated and validated against observed discharge data of the last century, and have compared projected discharge and flood frequencies in the twenty-first century with those of the last 100 years. However,

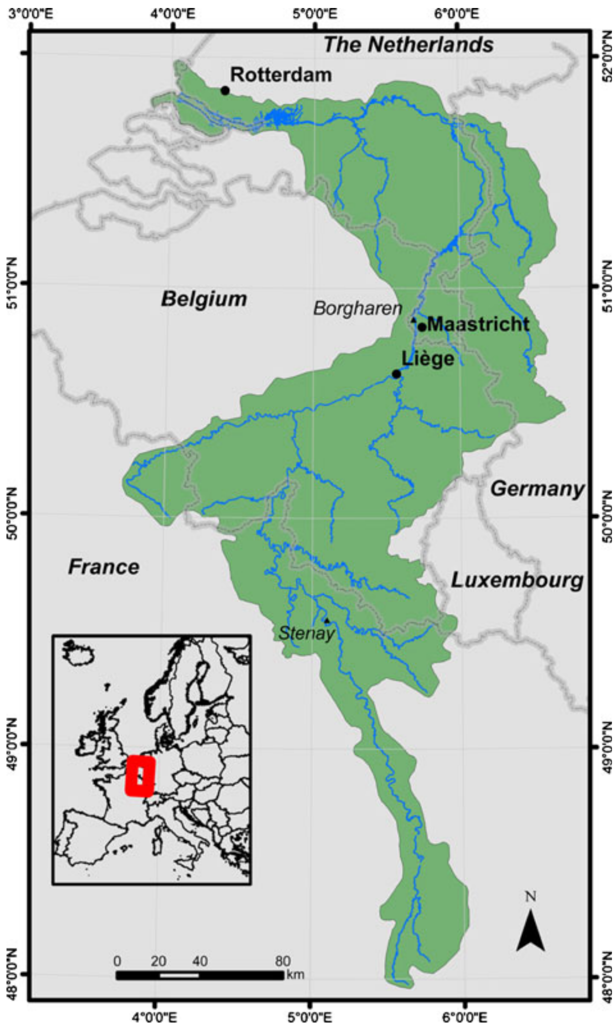

Fig. 1 Map showing the location of the Meuse Basin (after RWS Limburg/IWACO 2000). For this study the model was set up upstream from Borgharen. The *inset* shows the location of the Meuse basin in Europe

simulations of long-term changes (centuries to millennia) could help to understand the characteristics of natural decadal–centennial scale variability in discharge (Arnell et al. 2001), and to assess future changes in the context of natural variability. Ward et al. (2007) simulated the discharge of 19 river basins around the world on a monthly time-step for three periods during the Holocene, and Aerts et al. (2006) extended these simulations for the period 9000 BP until 2100 AD for 15 of the basins. The results of the latter study showed that mean river discharge in the majority of the basins is expected to change more due to climate change in the twenty-first century than due to natural climate variability over the last 9,000 years. These simulations were carried out with a monthly time-step, and only considered natural changes in land use in response to long-term climatic change. Ward et al. (2008) simulated the daily discharge of the Meuse over the periods 4000–3000 BP and 1000–2000 AD. The period 4000–3000 BP was selected as a natural reference period since the natural climatic forcings at that time were broadly similar to those of today (Goudie 1992), whilst human influence on land use was minimal (Bunnik 1995; Gotjé et al. 1990; RWS Limburg/IWACO 2000). The basin was heavily influenced by human activities in the period 1000–2000 AD, namely changes in land use throughout the period, and greenhouse gas and sulphate aerosol emissions since the industrial revolution. The results showed that the discharge and frequency of high-flows (up to 3,000 $m^3\ s^{-1}$) were higher in the period 1000–2000 AD than in the period 4000–3000 AD, mainly as a result of lower evapotranspiration due to the large-scale conversion of forest to agricultural land. However, despite reforestation over the last 100 years, discharge and the frequency of such high-flow events were higher in the twentieth century than in the nineteenth century. Almost all of this change can be explained by higher precipitation totals, particularly in the winter half-year (November–April). Hence, climate and land use have both had major effects on late Holocene Meuse discharge on different timescales. Assessments of the future effects of these factors would allow us to assess future change in the context of millennial scale natural and human-induced environmental change.

The aim of the present study is to assess the effects of projected climate and land use change in the twenty-first century on the discharge and flood frequency of the Meuse river, in relation to the effects of millennial scale natural and anthropogenic environmental changes over the course of the late Holocene. This will allow us to assess the nature and scale of future changes in discharge and flood frequency in the context of long-term (millennial) changes. To the best of our knowledge, this is the first hydrological modelling study to assess future changes in discharge and flood frequency in relation to long term changes during the late Holocene.

2 Study area

The Meuse is a predominantly rain-fed river with a total length of ca. 875 km, and a catchment area of ca. 33,000 km^2. For this study, the basin has been modelled upstream from Borgharen (Fig. 1). Borgharen is situated in the Netherlands, close to the Belgian–Dutch border; the catchment area upstream from Borgharen is ca. 21,000 km^2. The model was set up upstream from this point for a number of reasons. Firstly, discharge measurements at Borgharen, corrected for canal extractions upstream, are available since 1911, which is the longest discharge time-series in the basin, and allows for model calibration and validation. Secondly, current water management practice in the Netherlands uses daily discharge observations at Borgharen in the estimation of flood return periods. Thirdly, we did not model the basin as far downstream as the current Rhine-Meuse confluence, since its location has changed over the course of the Holocene (Berendsen and Stouthamer 2001). Mean annual precipitation over the basin is ca. 950 mm a^{-1}, and is reasonably evenly distributed throughout the year. The spatial distribution of precipitation is to a large extent a reflection of elevation and distance from the coast. Mean temperatures show marked seasonal variations, and annual potential evapotranspiration is much higher in the summer half-year (May–October) than in the winter half-year (November–April) (76% and 24% of the total respectively). The mean annual discharge of the Meuse and its associated canals at the border of Belgium and the Netherlands is ca. 276 m^3 s^{-1}; summer and winter half-year mean discharge are 146 and 406 m^3 s^{-1} respectively (Ashagrie et al. 2006).

3 Methods

Initially, the climate model ECBilt-CLIO-VECODE (Brovkin et al. 2002; Goosse and Fichefet 1999; Opsteegh et al. 1998) was coupled with the hydrological model STREAM (Aerts et al. 1999) to simulate Meuse palaeodischarge at a spatial resolution of $2' \times 2'$ with a daily time-step, for the periods 4000–3000 BP and 1000–2000 AD. Climate change was modelled in a transient manner, whilst land use configurations were changed in time steps of one century (Ward et al. 2008). In the present study, the experiment was subsequently continued until 2100 AD.

3.1 Models and climate forcing parameters

ECBilt-CLIO-VECODE is a three-dimensional coupled climate model consisting of three components describing the atmosphere, ocean, and vegetation (Brovkin et al. 2002; Goosse and Fichefet 1999; Opsteegh et al. 1998). The model is an Earth System Model of Intermediate Complexity (EMIC) (Claussen et al. 2002). The atmospheric model ECBilt is a quasi-geostrophic, T21 horizontal resolution spectral model, corresponding to a horizontal resolution of ca. $5.6° \times 5.6°$, with three vertical levels (Opsteegh et al. 1998). CLIO is a primitive-equation three-dimensional, free-surface ocean general circulation model coupled to a thermodynamic and dynamic sea-ice model, and has a horizontal resolution of $3° \times 3°$, with 20 vertical levels (Goosse and Fichefet 1999). The dynamic terrestrial vegetation model VECODE computes herbaceous plant, tree, and desert fractions per land grid cell (Brovkin et al. 2002) and is coupled to ECBilt through the surface albedo.

The climate model output used in this study were forced by annually varying orbital parameters following Renssen et al. (2005); atmospheric volcanic aerosol content and fluctuations in solar activity following Goosse et al. (2005); and atmospheric greenhouse gas and sulphate aerosol concentrations following Renssen et al. (2005) for 4000–3000 BP and 1000–1750 AD, and Goosse et al. (2005) for 1750–2000 AD. For the twenty-first century, atmospheric volcanic aerosol content and fluctuations in solar activity were assumed to have the same values as for the twentieth century (Goosse et al. 2005) in order to facilitate comparisons between the twentieth and twenty-first centuries, and atmospheric greenhouse gas and sulphate aerosol concentrations were prescribed according to the Special Report on Emission Scenarios (SRES) of the Intergovernmental Panel on Climate Change (IPCC 2000). We used SRES emission scenarios A2 and B1 since these lie towards the upper and lower end of the full spectrum of IPCC scenarios respectively in terms of projected temperature change by the end of the twenty-first century, and can therefore be used to assess the response of the system to a broad range of possible future changes. Compared to the baseline concentration of atmospheric CO_2 in 1990 AD (ca. 354 ppm), the A2 and B1 scenarios prescribe increases to 836 and 540 ppm respectively by 2100 AD. The climate model experiments were run in ensemble mode, with four ensemble members. Each ensemble member represents a single model run. The ensemble members are forced using the same climatic parameters, but with slightly different initial climatic conditions to account for the chaotic behaviour of the atmospheric system. Hence, the ensemble mean can be used to evaluate long-term trends and changes.

STREAM is a grid-based spatially distributed water balance model that describes the hydrological cycle of a drainage basin as a series of storage compartments and flows (Aerts et al. 1999). It is based on the RHINEFLOW model of Kwadijk (1993), and uses a raster GIS database to calculate the water balance of each grid cell per time-step. The water balance is calculated using the Thornthwaite (1948) equations for potential evapotranspiration and the Thornthwaite and Mather (1957) equations for actual evapotranspiration; these equations use temperature and precipitation as the major input parameters. For each time-step the model generates runoff, groundwater storage (shallow and deep), snow cover, and snow melt. The direction of water flow between cells is based on the steepest descent for the eight surrounding grid cells on a digital elevation model (DEM). The main flows and storage compartments used to calculate water availability per cell are shown in Fig. 2.

In this study, STREAM is run with a daily time-step, and a spatial resolution of $2' \times 2'$ (ca. 2.4 km × 3.7 km); this is high enough to capture the dominant processes in the basin (Booij 2002). We derived the flow network based on the USGS GTOPO30 DEM (http://edc.usgs.gov/products/elevation/gtopo30/gtopo30.html). The model was forced using all four ensemble members of the climate model data.

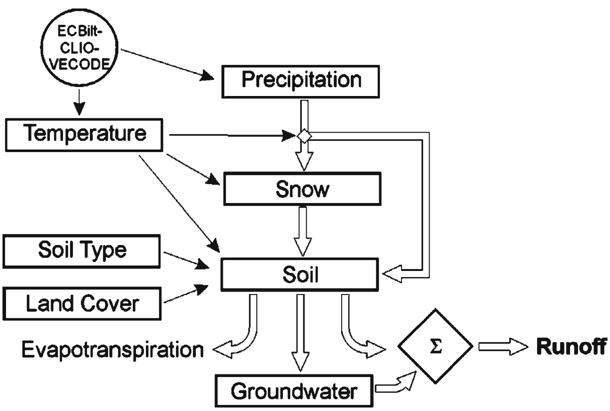

Fig. 2 Flowchart showing the main storage compartments and flows of the STREAM palaeodischarge model

3.2 Climate input data

The climate data (daily temperature and precipitation) derived from ECBilt-CLIO-VECODE have a spatial resolution of ca. 5.6° × 5.6°, and therefore need downscaling to the resolution of the STREAM model (2′ × 2′). The first step was a spatial downscaling procedure (Bouwer et al. 2004), whereby the values from the ca. 5.6° × 5.6° climate model grid were simply resampled onto a 2′ × 2′ grid. We then applied correction factors to the spatially downscaled climate model data (for temperature additive and for precipitation multiplicative), which were derived from the difference for each grid cell in mean monthly temperature and precipitation between the climate model data and a higher resolution baseline dataset. For the baseline dataset we used the CRU TS 1.2 dataset of precipitation and temperature (Mitchell and Jones 2005), which has a spatial resolution of 10′ × 10′.

The spatially downscaled ECBilt-CLIO-VECODE data were spatially redistributed using the following formulae:

$$p'_{ECB(d,i)} = p_{ECB(d,i)} \times \left(\frac{\bar{P}_{CRU(m,i)}}{\bar{P}_{ECB(m,i)}} \right) \tag{1}$$

where $p'_{ECB(d,i)}$ is the spatially redistributed ECBilt precipitation for a particular day, d, and cell, i, $p_{ECB(d,i)}$ is the raw ECBilt precipitation for a particular day, d, and cell, i, $\bar{p}_{CRU(m,i)}$ is the observed (CRU) average monthly precipitation for a particular month, m, and cell, i, and $\bar{p}_{ECB(m,i)}$ is the raw ECBilt mean monthly precipitation for a particular month, m, and cell, i.

$$t'_{ECB(d,i)} = t_{ECB(d,i)} + \left(\bar{t}_{CRU(m,i)} - \bar{t}_{ECB(m,i)} \right) \tag{2}$$

where $t'_{ECB(d,i)}$ is the spatially redistributed ECBilt temperature for a particular day, d, and cell, i, $t_{ECB(d,i)}$ is the raw ECBilt temperature for a particular day, d, and cell, i, $\bar{t}_{CRU(m,i)}$ is the observed average monthly temperature for a particular month, m, and cell, i, and $\bar{t}_{ECB(m,i)}$ is the raw ECBilt mean monthly temperature for a particular month, m, and cell, i. An analysis of the agreement between the downscaled and observed datasets of precipitation and temperature can be found in Ward et al. (2008).

3.3 Land use input data

A crop factor map is used in STREAM to calculate potential evapotranspiration (PE). The crop factor is a dimensionless factor by which the reference PE is multiplied in order to account for the difference in PE over different land use types. The land use classes were simplified due to the relative scarcity of detailed historical land use data, and reclassed to crop factor maps based on values in Kwadijk (1993), and Aerts and Bouwer (2002): urban (0.8); forests (1.1); agriculture and grasslands (0.9); wetlands (1.1); and water bodies (1.5). In this section we describe the land use input data used for the twentieth and twenty-first century simulations. The land use data used for the preceding periods (i.e. 4000–3000 BP and 1000–1900 AD) are discussed in detail in Ward et al. (2008).

Land use configurations for the twentieth and twenty-first centuries were based on the EURURALIS 2.0 project (WUR/MNP 2007; www.eururalis.eu). For the twentieth century, the land use configuration was based on the situation in 2000 AD. For the twenty-first century, the land use configuration was based on the projected situation following the scenarios 'Continental Market' and 'Global Cooperation', which correspond with the climate emission (SRES) scenarios A2 and B1 respectively. Throughout the rest of this paper we therefore refer to these land use scenarios as A2 and B1. However, since the focus of the SRES scenarios (IPCC 2000) is outside land use, agriculture, and rural development, and lacks the regional disaggregation needed for high resolution land use modelling (Verburg et al. 2006), the EURURALIS scenarios were elaborated for land use issues and agricultural policies typical for Europe (Westhoek et al. 2006). Future land use change was simulated with an extended version of the global economic model (GTAP) and an integrated assessment model (IMAGE) to calculate changes in demand for agricultural area at the country level, whilst a spatially explicit land use change model (CLUE-s) was used to translate these land claims into land use patterns at a 1 km × 1 km resolution (Verburg et al. 2006, 2008). Since land use change is dependent on physical, socioeconomic, and political processes (such as changes in the common agricultural policy, oil prices, etc.) (Van Rompaey et al. 2002; Verburg 2006), it is difficult to simulate meaningful scenarios for long timeframes, and therefore the results are highly sensitive to future socioeconomic and political decisions and preferences. Therefore, the land use simulations of the EURURALIS project were made based on anticipated changes in the main drivers of land use change assumed to be valid for the year 2030 AD. The projected land use situation for 2030 AD was assumed to be representative for the first half of the twenty-first century (2000–2050 period). In the analysis a direct comparison with the results for 4000–3000 BP and 1000–2000 AD is made, as the land use scenarios were also changed in time-steps of one century in these periods.

3.4 Calibration and validation of the STREAM model

Calibration was carried out for the relatively wet period 1961–2000, and validation for the relatively dry period 1921–1960. The calibration was initially carried out for the main river at Borgharen, using data provided by RWS Waterdienst, pertaining to the 'undivided Meuse'; they are based on discharge measurements at Borgharen, corrected for canal extractions between Liège and Borgharen (De Wit et al. 2007b), and are available since 1911. Observed data from ten gauging stations further upstream were also used. The calibration was carried out by varying model parameters with the aim of reproducing daily, monthly, and annual discharge characteristics similar to those of the observed records. Where independent measurements exist for output variables other than discharge, these were also used in the calibration; in this case actual evapotranspiration (AE) and the number of snow-cover days. The results of the calibration and validation, as well as sensitivity analysis, are discussed in Ward et al. (2008).

4 Results

4.1 Land use change

The basin-average land use (upstream from Borgharen) is given in Table 1. It should be noted that the land use for the twenty-first century is in fact a projection

Table 1 Land use upstream from Borgharen, shown as a percentage of total area

Land use class	Time-period				
	4000–3000 BP	1000–2000 AD	20th century	21st century (A2)	21st century (B1)
Urban	0.0%	1.1%	9.7%	10.3%	10.3%
Forests	97.6%	40.8%	34.7%	34.6%	36.6%
Agriculture and grasslands	0.0%	56.2%	54.7%	54.6%	52.6%
Other	2.4%	1.9%	0.9%	0.5%	0.5%

For the period 1000–2000 AD, the land use configuration was altered per 100 year period; the value shown here represents the average configuration over the entire period

to 2030 AD only, thus likely underestimating the changes for the entire century. The overall change in land use between the twentieth century and 2030 AD is small for the A2 scenario. This scenario depicts a world of divided regional blocks in which each block strives for self sufficiency so as to be less reliant on other blocks. Agricultural trade barriers and support mechanisms continue to exist. In combination with high economic growth in the region, claims on land resources are high for both urbanisation and agriculture. As a result, the agricultural area faces little change. In spite of the low net changes there are some shifts in land use patterns: marginal, low intensity grasslands on the steep slopes of the Belgian Ardennes are reforested, whilst some patches of forest in the areas more suitable for agriculture (on the plateaus and the margins of the region) are reclaimed for agriculture.

Under the B1 scenario, the forested area at 2030 AD is higher than in the twentieth century by ca. 2%, whilst the area under agriculture and grassland is lower by ca. 2%. The B1 scenario depicts a world of successful international cooperation aimed at poverty reduction and environmental protection. Trade barriers are removed and governance aims at protecting cultural and natural heritage values. Increased global trade in agricultural commodities, in combination with increased productivity, leads to lower claims on agricultural lands in marginal areas, such as large parts of the Meuse basin. As crops can be produced much more efficiently in other regions of Europe (and the rest of the world), large areas of arable land in the Meuse catchment could potentially be abandoned or reforested. However, at the same time it is assumed that under this scenario subsidies for farmers in less suitable areas are maintained, and since most of the Meuse basin is eligible for such subsidies, land abandonment is reduced to a large extent.

In both scenarios, the rate of urbanisation is rather low. This is mainly due to the limited number of major cities located in the catchment, and the catchment's location outside the core economic regions of the riparian countries. Large areas of agricultural land in western Belgium (outside the Meuse basin) are converted to urban area; this loss of prime agricultural land provides another incentive for farmers in the eastern part of the country (where the Meuse catchment is situated) to continue farming.

4.2 Long-term trends and changes in climate and discharge

The long-term changes in mean 50-year discharge at Borgharen, and basin-averaged mean temperature and precipitation per 50-year period, are shown in Fig. 3; in these

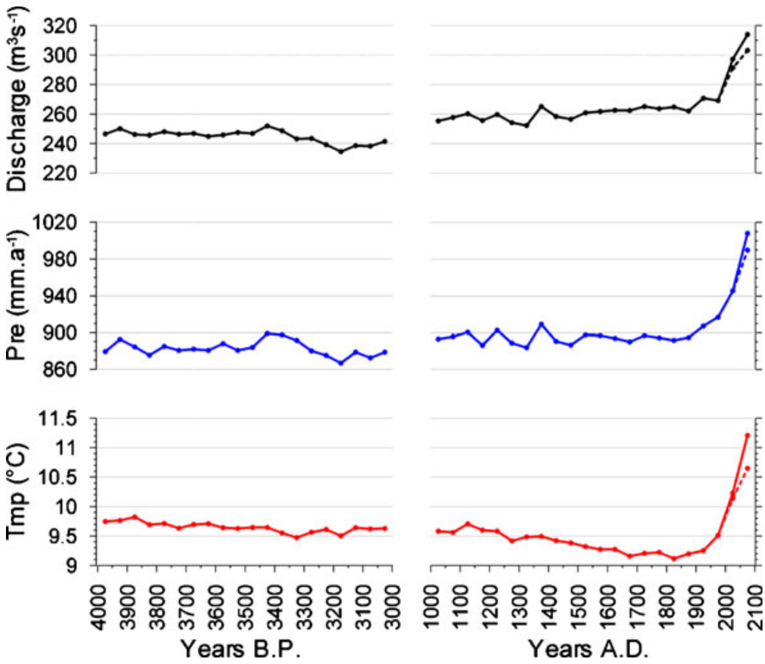

Fig. 3 Long-term changes in mean annual discharge at Borgharen, basin-averaged precipitation (*pre*), and basin-averaged temperature (*tmp*). The combined means of the four ensemble members are shown for each 50-year period. For the twenty-first century, the A2 scenario is shown as an *unbroken line* (*upper*), and the B1 scenario as a *dotted line* (*lower*)

simulations the twenty-first century experiments are carried out using the A2 and B1 climate and land use configurations, which show projections of land use until 2030 AD only. Hence, the effects of land use change in the second half of the twenty-first century are not included in the simulation. Throughout this paper we have used the Mann–Kendall (MK) test to assess the statistical significance of trends over different periods, and the t-test to assess the statistical significance of changes in mean values between different periods.

Over the course of the period 4000–3000 BP, mean 50-year temperature shows a statistically significant negative trend ($p < 0.001$; Fig. 3). This trend is also evident over the period 1000–1900 AD ($p < 0.001$). However, after 1850 AD, the curve of mean temperature (Fig. 3) shows a positive trend under both the A2 and B1 scenarios, to temperatures far higher than those in any other period studied.

Whilst mean 50-year precipitation shows no significant trend over the periods 4000–3000 BP or 1000–2000 AD ($p = -0.1048$ and $p = -0.2176$ respectively), mean precipitation is significantly higher in 1000–2000 AD than in 4000–3000 BP ($p < 0.001$) (Fig. 3). There is a positive trend in mean precipitation after 1850 AD (Fig. 3). The mean precipitation in the period 1950–2000 AD (917.2 mm a^{-1}) is higher than in any preceding 50-year period, and is higher still in the twenty-first century, reaching ca. 1008.1 mm a^{-1} (A2) or 989.9 mm a^{-1} (B1) for the period 2050–2100 AD.

The effects of the prescribed changes in climate and land use on discharge are also shown in Fig. 3. Mean 50-year discharge is significantly higher ($p < 0.001$)

in the period 1000–2000 AD (261.0 m^3 s^{-1}) than in the period 4000–3000 BP (244.8 m^3 s^{-1}). Furthermore, mean discharge shows a significant positive trend over the period 1000–2000 AD ($p < 0.001$). In the twenty-first century, mean discharge is much higher than during any other 50-year period in the time-periods studied. For the period 2050–2100 AD, mean discharge is 314.0 m^3 s^{-1} (A2) or 303.3 m^3 s^{-1} (B1).

4.3 Relative contributions of climate and land use change to changes in discharge

In this section we examine the impacts of climate and land use change on Meuse discharge (annual and seasonal) and medium-sized high-flow events on different timescales. In Table 2, we show the percentage change in mean annual, summer, and winter discharge, as well as a number of high-flow percentiles, between the periods 1950–2000 AD and 2000–2050 AD. These changes are based on the combined model results for all four climate model ensemble members, thereby increasing the length of the discharge series for each 50 year period to 200 years. The results are shown for these two periods of half a century only, since the land use data for the twenty-first century refer only to the situation in 2030 AD, thereby providing a better representation of the average land use in the period 2000–2050 AD than of the average land use over the entire twenty-first century. The t-test was carried out on the annual values for each parameter based on the combined results of the four climate model ensemble members. The combined effects of climate and land use change on annual and seasonal discharge, as well as medium-sized high-flows (Q_{90}, Q_{95}, Q_{99}) result in significantly higher values in the period 2000–2050 AD than in the period 1950–2000 AD (Table 2).

In order to assess the relative contribution of changes in climate and land use to changes in these discharge parameters, we carried out further simulations with STREAM, but using the land use configuration of the twentieth century in combination with the climate data for 2000–2050 AD, and the land use configuration representative for the first half of the twenty-first century in combination with the climate data for 1950–2000 AD. In this way the effects of changes in climate and

Table 2 Percentage change in absolute values of mean annual (Q_{ann}), summer half-year (May–October) (Q_{sum}), and winter half-year (November–April) (Q_{win}) discharge and various high-flow percentiles (Q_k, k = 90, 95, 99) between the periods 1950–2000 and 2000–2050 under scenario A2 (above) and B1 (below)

	Q_{ann}	Q_{sum}	Q_{win}	Q_{90}	Q_{95}	Q_{99}
Percentage change between 1950–2000 and 2000–2050 (A2 scenario)						
Climate and land use	*+10.5*	*+8.2*	*+11.3*	*+9.6*	*+8.3*	*+7.1*
Climate only	*+10.4*	*+8.4*	*+11.1*	*+9.6*	*+8.6*	*+8.4*
Land use only	0.0	−0.2	+0.1	0.0	−0.3	−1.4
Percentage change between 1950–2000 and 2000–2050 (B1 scenario)						
Climate and land use	*+8.2*	*+3.1*	*+10.0*	*+8.6*	*+8.6*	*+6.3*
Climate only	*+8.8*	*+4.6*	*+10.3*	*+9.0*	*+9.2*	*+7.9*
Land use only	−0.6	−1.5	−0.3	−0.4	−0.6	−1.6

Changes with statistical significance (t-test, $\alpha = 0.05$, n = 200) (50 years × four ensemble members) are shown in italics. The t-test was carried out on the annual values for each parameter by combining the results of the four climate ensemble members land use were delineated; the results are also shown in Table 2. For both scenarios, the effects of land use change alone are small, and the only notable effect is a minor dampening of the large increase forced by the change in climate. The small land use changes simulated by the EURURALIS land use model have very minor effects on Meuse discharge. It should be noted that the effects of land use change, as simulated in this study, only pertain to changes in the crop factor resulting from changes in land use. Changes in land use intensity or water management measures (e.g. water retention areas) may have a greater influence on discharge.

We also carried out a similar exercise to assess the relative effects of changes in climate and land use change on discharge between the natural reference period 4000–3000 BP and the period 2000–2050 AD; the results are shown in Table 3. For both scenarios, the effects of climate and land use change on mean annual discharge are of a similar order of magnitude on this timescale; the effects of land use change are stronger in the summer half-year, whilst the effects of climate change are stronger in the winter half-year. Changes in both climate and land use have led to significantly higher values of the high-flow percentiles shown here for the period 2000–2050 AD, compared to those for the natural reference period (4000–3000 BP).

4.4 Trends and changes in climate and their impacts on discharge in the twentieth and twenty-first centuries

The long-term simulations of temperature, precipitation, and discharge all suggest large increases over the coming century, resulting in values greater than those seen over the last 4,000 years. In this section we examine the trends and changes in climate in the twentieth and twenty-first centuries, and their impacts on discharge in more detail. Since the impact of the projected small changes in land use between 1950–2000 AD and 2000–2050 AD on mean discharge is minor, and we have no projections of land use change for the latter half of the twenty-first century, we use a

Table 3 Percentage change in mean annual (Q_{ann}), summer half-year (May–October) (Q_{sum}), and winter half-year (November–April) (Q_{win}) discharge and various high-flow percentiles (Q_k, k = 90, 95, 99) between the periods 4000–3000 BP and 2000–2050 AD under scenario A2 (above) and B1 (below)

	Q_{ann}	Q_{sum}	Q_{win}	Q_{90}	Q_{95}	Q_{99}
Percentage change between 4000–3000 BP and 2000–2050 (A2 scenario)						
Climate and land use	+23.3	+37.6	+19.1	+16.1	+14.5	+10.4
Climate only	+10.9	+10.1	+11.1	+9.5	+8.9	+6.0
Land use only	+12.4	+27.5	+8.0	+6.6	+5.5	+4.4
Percentage change between 4000–3000 BP and 2000–2050 (B1 scenario)						
Climate and land use	+20.8	+31.1	+17.7	+15.1	+14.8	+9.6
Climate only	+9.1	+5.5	+10.2	+8.8	+9.5	+5.4
Land use only	+11.7	+25.6	+7.6	+6.3	+5.2	+4.3

On this timescale the effects of climate and land use change on mean annual discharge have been of a similar order of magnitude; the effects of land use change have been stronger in the summer half-year, whilst the effects of climate change have been stronger in the winter half-year. For all of the discharge percentiles shown here, both changes in climate and land use have caused changes with statistical significance (t-test, $\alpha = 0.05$, $n = 200$) (50 years $\times$ four ensemble members). The t-test was carried out on the annual values for each parameter by combining the results of the four climate ensemble members constant land use scenario, namely that of the twentieth century. Hence, the 10-year running means for temperature, precipitation, actual evapotranspiration (AE), and discharge, in the period 1900–2100 AD given in Fig. 3, are forced only by changes in climatic parameters. The results are shown per season, i.e. winter (December, January, February), spring (March, April, May), summer (June, July, August), and autumn (September, October, November), and are the combined results for the four climate model ensemble runs. For the twenty-first century, the results of the MK test to detect monotonic trends are shown in Table 4.

Over the course of the twentieth century, annual mean, summer half-year, and winter half-year temperature all show significant positive trends (Ward et al. 2008). This is also the case for the twenty-first century under both scenarios, and for all seasons (Table 4). Mean annual temperature in the period 2050–2100 AD is 1.7°C (A2) or 1.1°C (B1) higher than in the period 1950–2000 AD. The resulting mean annual temperature for the period 2050–2100 AD under the A2 scenario (ca. 11.2°C) is significantly higher than that under scenario B1 (10.7°C; $p < 0.001$).

Over the course of the twenty-first century, there are significant positive trends of mean annual precipitation under both scenarios (Table 4). This is also the case for the winter, spring, and autumn, with the strongest trend in winter (Fig. 4b and Table 4). Summer precipitation is lower in the period 2050–2100 AD for both scenario A2 (226.2 mm a^{-1}) and B1 (236.3 mm a^{-1}) than in the period 1950–2000 (238.2 mm a^{-1}), although this decrease is not statistically significant in either case ($p = 0.070$ and $p = 0.752$ for A2 and B1 respectively). Mean annual precipitation in the period 2050–2100 AD is significantly higher than in the period 1950–2000 AD, with an increase of 91 mm a^{-1} (A2) or 73 mm a^{-1} (B1). For both scenarios, there is no change in the interannual variability of precipitation during any season (F-test, $\alpha = 0.05$), except for an increased variability during the spring under scenario A2.

Table 4 Results of the Mann–Kendall (MK) test to assess the presence or absence of a monotonic trend (in temperature, precipitation, actual evapotranspiration (AE), and discharge) over the course of the twenty-first century

Period	Annual		Winter		Spring		Summer		Autumn	
	MK	p	MK	p	MK	p	MK	p	MK	p
A2 scenario										
Temperature	11.92	*<0.001*	12.23	*<0.001*	10.43	*<0.001*	8.71	*<0.001*	10.67	*<0.001*
Precipitation	4.96	*<0.001*	6.53	*<0.001*	7.61	*<0.001*	−1.83	0.067	5.84	*<0.001*
AE	5.81	*<0.001*	12.24	*<0.001*	10.33	*<0.001*	−1.60	0.109	4.75	*<0.001*
Discharge	2.91	*0.004*	4.34	*<0.001*	1.96	*0.049*	1.96	*0.049*	0.42	0.671
B1 scenario										
Temperature	9.30	*<0.001*	9.13	*<0.001*	7.29	*<0.001*	5.69	*<0.001*	7.43	*<0.001*
Precipitation	4.8	*<0.001*	4.14	*<0.001*	5.68	*<0.001*	1.07	0.284	3.19	*<0.001*
AE	6.02	*<0.001*	9.12	*<0.001*	7.65	*<0.001*	1.643	0.100	4.55	*<0.001*
Discharge	3.20	*0.001*	3.82	*<0.001*	1.02	0.306	1.99	*0.047*	1.51	0.130

A positive MK statistic represents a positive trend, whilst a negative MK statistic represents a negative trend. Probabilities with statistical significance ($\alpha = 0.05$) are shown in italics. The results are shown for mean annual values, as well as values for winter (December, January, February), spring (March, April, May), summer (June, July, August), and autumn (September, October, November)

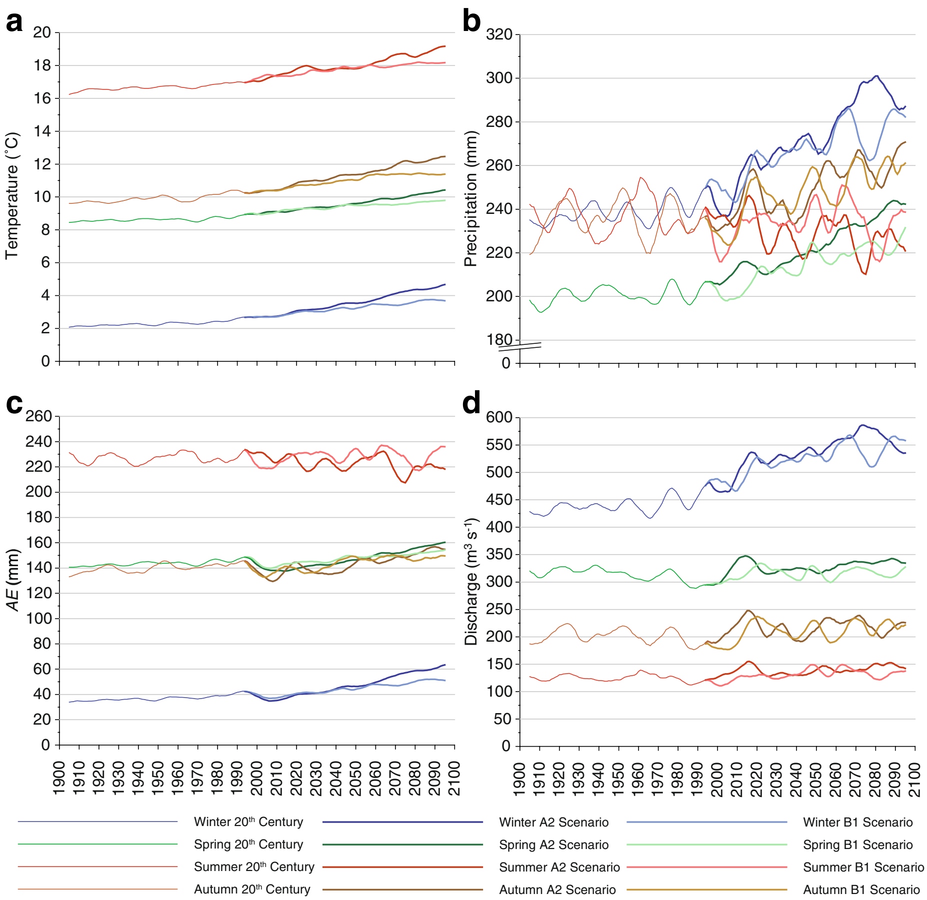

Fig. 4 Combined 10-year running means of the four ensemble members for basin-averaged **a** temperature, **b** precipitation, and **c** actual evapotranspiration (AE), and for **d** mean discharge at Borgharen. The results are shown for winter (December, January, February), spring (March, April, May), summer (June, July, August), and autumn (September, October, November)

The interactions of temperature and precipitation, and their impact on soil moisture content, lead to alternations in actual evapotranspiration (AE). As a result of the positive trend in temperature over the course of the twentieth century, mean annual and winter half-year AE also show significant positive trends over that time-period. For the twenty-first century, the positive trends in annual temperature and precipitation also lead to a strong and positive trend in AE (Table 4); this is also the case for all seasons except for summer, for which there is no significant trend under either scenario. This can be explained by two factors: (a) summer season precipitation is lower in the period 2050–2100 AD than in 1950–2000 AD; and (b) the results show that, on average, the soil moisture storage compartment of the hydrological model holds less water in the summer season in the twenty-first century than in the twentieth century, as a result of higher AE in the preceding spring season.

Hence, less soil water moisture is available for evaporation, and surface runoff generation in the summer months is delayed since more precipitation is required to fill the soil moisture compartment.

No significant trends in either annual, summer half-year, or winter half-year discharge are found over the course of the twentieth century (Ward et al. 2008). For the twenty-first century, there is a clear positive trend in mean annual discharge (Table 4) under both scenarios. Mean annual discharge in the period 2000–2050 AD ($A2 = 297.4\ m^3\ s^{-1}$; $B1 = 293.1\ m^3\ s^{-1}$) is significantly higher than in the period 1950–2000 AD ($269.2\ m^3\ s^{-1}$; $p < 0.001$). In the period 2050–2100 AD, mean discharge is even higher ($A2 = 314.0\ m^3\ s^{-1}$, $B1 = 305.1\ m^3\ s^{-1}$). The higher mean annual discharge in the twenty-first century (compared to the twentieth century) is mainly the result of higher winter season discharge (Fig. 4d). Nevertheless, mean discharge is significantly higher for all seasons in the period 2050–2100 AD, when compared to the period 1950–2000 AD ($\alpha = 0.05$). Summer season discharge in the period 2050–2100 AD is $142.9\ m^3\ s^{-1}$ (A2) or $135.6\ m^3\ s^{-1}$ (B1), compared to $125.2\ m^3\ s^{-1}$ in the period 1950–2000 AD. This is despite the fact that: (a) mean summer precipitation is lower in 2050–2100 AD than in 1950–2000 AD by 12 mm (A2) or 2 mm (B1); and (b) there is no significant change in AE between those periods. Hence, the changes in discharge cannot be attributed to precipitation change alone. The model results reveal that the higher discharge in the summer months is caused by higher precipitation totals during the preceding spring, winter, and autumn, which lead to higher values of groundwater storage in the summer. As a result, the baseflow is higher in the twenty-first century than in the twentieth century, and this more than compensates for the lower modelled values of surface flow.

4.5 Flood events

In this section, we examine changes in the frequency of flood events over the late Holocene. For this purpose, we compare the frequency distributions of daily discharge for the periods 4000–3000 BP, 1000–2000 AD, and the 21st century. Since we only have future land use projections until the year 2030 AD, and do not know how this will change after that time, the twenty-first century results are based on a simulation using the constant twentieth century land use configuration. Hence, the changes between the twentieth and twenty-first century are forced by changes in climatic parameters only. The empirically derived frequency distributions of daily discharge are based on the combined results of the four climate model ensemble members, and hence the number of data-points for the 1,000 year periods is 4000, and the number of data-points for the 100 year periods is 400. There is a significant difference in the frequency distributions of daily discharge between the periods 4000–3000 BP and 1000–2000 AD, and also between 1000–2000 AD and the twenty-first century (Kolmogorov-Smirnov (KS) test, $p < 0.001$). In Fig. 5, we show the probability of daily discharge above a threshold, based on the results derived from STREAM. The frequency of high-flow events during the twenty-first century is higher than during the natural reference period 4000–3000 BP, the period 1000–2000 AD, and the twentieth century (under both scenarios A2 and B1). Floods with a magnitude of $3{,}000\ m^3\ s^{-1}$ (similar in magnitude to the major floods of 1926 and 1993) occur under scenario A2 twice as frequently as in the twentieth century, and almost four times as frequently as during the natural reference period 4000–3000 BP.

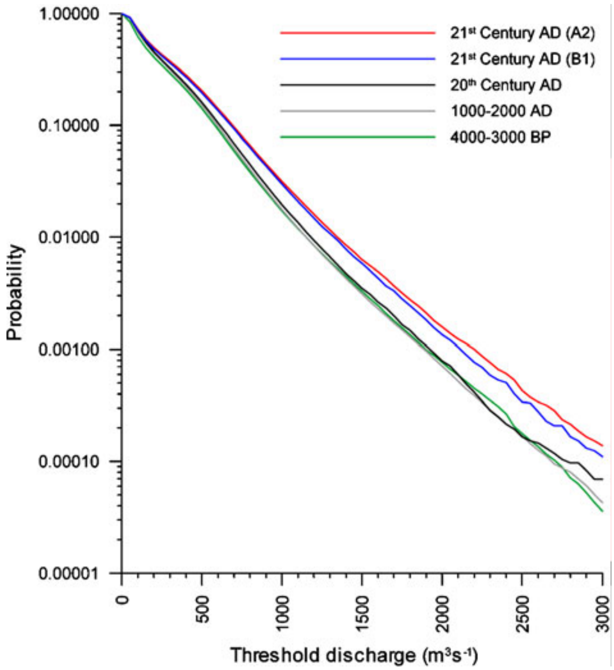

Fig. 5 Probability of daily discharge over a threshold. High-flow events of Q > 3,000 m^3 s^{-1} (similar in magnitude to the major floods of 1926 and 1993) are predicted more frequently in the twenty-first century than in any of the preceding time-periods shown, with the greatest increase under scenario A2

In order to assess the change in the frequency of extreme flood events, the use of extreme value statistics was required, since these events occur much less frequently than the length of the modelled time-series. Using the combined results of the four climate model ensemble members, we first assessed the quality of fit of several extreme value distributions (Gamma, GEV, Gumbel, Johnson, Lognormal, Pareto, Weibull) against the modelled data for the periods 4000–3000 BP, 1000–2000 AD, and the twenty-first century, using the KS and χ^2 tests; we found that the Gumbel distribution gave the best overall fit.

We then fit Gumbel distributions to each of the time-periods studied, and used these to estimate the magnitude of flood events with extremely long return periods. In Table 5, the discharge magnitudes associated with flood events with a return period of 1,250 years are shown. This return period was used since the design discharge for embanked sections of the Netherlands is also based on an event with this return period. However, it should be noted that the method used to determine the design discharge is different to the one used here (a weighted average of several extreme discharge distributions is used in the official assessment of design discharge; Diermanse 2004), and hence our results should not be interpreted as alternative estimates of design discharge. There is little variation in the discharge magnitude associated with a return period of 1,250 years between the periods 4000–3000 BP, 1000–2000 AD, and the twentieth century (Table 5). However, for the twenty-first century, the magnitude of the flood with return period of 1,250 years is higher than for the preceding time-periods, especially for scenario A2, which falls outside the upper 95% confidence limit of the twentieth century estimate. The results in Table 5 also show that the effects of land use change on the magnitude of such extreme events

Table 5 Discharge magnitude associated with a flood event with return period 1,250 years

Simulation	Discharge ($m^3 s^{-1}$)
Observed discharge (1912–2000 AD)	4,112
20th century	4,137
20th century (lower/upper 95% confidence limits)	3,857/4,416
4000–3000 BP	4,093
1000–2000 AD	4,073
21st century (A2: climate only)	4,617
21st century (B1: climate only)	4,357

These magnitudes are obtained by fitting a Gumbel distribution to the values of annual maximum discharge. The values presented in the table are based on the simulation results for all four ensemble members. The value for observed discharge is based on the observed annual maximum discharges at Borgharen for the period 1912–2000 AD. The values for the twenty-first century are estimated using the twenty-first century climate, but the twentieth century land use configuration. For the twentieth century simulations, the discharge magnitude associated with the upper and lower 95% confidence limits of the Gumbel distribution are also shown; for the twenty-first century the discharge magnitude falls outside these limits under the A2 scenario

are small, with little change between the periods 4000–3000 BP and 1000–2000 AD, despite a reduction in forest cover of more than 50%.

5 Discussion

5.1 Effects of long-term changes in climate and land use on past and future Meuse discharge

The discharge and the frequency of medium-sized high-flows (e.g. Q_{99}) of the Meuse are significantly higher in the period 1000–2000 AD than in the natural reference period 4000–3000 BP; on this millennial timescale almost all of the increase is the result of decreased evapotranspiration due to the conversion of forest to agricultural land. However, despite a large increase in forested area between the nineteenth and twentieth centuries, discharge and medium-sized high-flow frequency are greater in the latter period than in the former; these increases are attributable to a large increase in (winter half-year) precipitation (Ward et al. 2008).

The results of the present study suggest that the long-term trend of increasing mean discharge will continue and strengthen throughout the twenty-first century. In the first half of the twenty-first century (2000–2050 AD), the discharge and frequency of medium-sized high-flows are significantly higher than in the preceding half century (1950–2000 AD). Despite the theoretical potential of changes in forest cover to significantly alter mean discharge and flood magnitudes (as exemplified by the effects over the late Holocene), the projected changes in land use between 1950–2000 AD and 2000–2050 AD are small. As a result, the effects of land use change have little effect on discharge and high-flow frequency on this timescale. In the period 2000–2050 AD, the difference in discharge between the A2 and B1 scenarios is small; the difference is greater in the period 2050–2100 AD. This is logical since the expected emissions of greenhouse gases under SRES emission scenarios A2 and B1 diverge more greatly during the second half of the twenty-first century.

Despite the fact that land use change during the first half of the twenty-first century may have little effect on the mean discharge and medium-sized high-flow frequency of the Meuse, the effects of climate and land use change on mean discharge have been of a similar order of magnitude if we compare the periods 4000–3000 BP and 2000–2050 AD. The effects of land use change have been stronger in the summer half–year, and the effects of climate change stronger in the winter half-year. This difference can be explained by the fact that: (a) the increase in winter half-year precipitation between those time periods is greater than the increase in summer half-year precipitation; and (b) the large-scale conversion of forest to agricultural land between the natural reference period 4000–3000 BP and 2000–2050 AD has resulted in lower values of PE in the latter period. Clearly, this difference is greater in the summer half-year than in the winter half-year, since most evapotranspiration takes place in the summer half-year.

Nevertheless, even on the millennial timescale the deforestation of almost half of the basin has had little effect on extreme flood events (in this case operationalised by events with a return period of 1,250 years). Whilst numerous studies of the effects of deforestation on flood events have shown increased peak-flows around the globe (e.g. Brown et al. 2005; Gentry and Parody 1980; Jones 2000; Mahe et al. 2005), reviews of paired catchment studies show that this is not always the case (Andréassian 2004; EEA 2001). Cosandey et al. (2005) state that the effects of deforestation on flood generation are less severe during large-scale, low intensity (frontal) rainfall events. The most severe flood events on the Meuse occur as a result of extended periods of frontal rainfall over large parts of the basin (Berger 1992). Since the most extreme rainfall events of such a nature occur in the Meuse basin during the winter, our results show that the combination of saturated soils associated with a long period of antecedent precipitation, and low evapotranspiration rates during the winter, combine to minimise the effects of changes in forest cover on the most extreme flood events.

5.2 Comparison with other studies

Reconstructions of temperature, precipitation, and discharge, based on geological and geomorphological proxy data in the Meuse basin and northwest Europe, provide qualitative indications of the signs of change in these parameters over the course of the late Holocene. The main trends of these findings are generally in agreement with our results. Multi-proxy reconstructions of regional temperature for the late Holocene show a gradual decrease in temperature (especially in summer)(Bohncke et al. 1987; Goosse et al. 2006; Zagwijn 1994). Proxy data on late Holocene precipitation change in the region are scarce, but suggest slightly higher precipitation totals in the last millennium compared to the period 4000–3000 BP (Bohncke and Vandenberghe 1991; Van Geel et al. 1996). Multi-proxy studies on late Holocene discharge in the Meuse basin are in general agreement with our conclusion of increasing mean discharge and high-flows (e.g. Berendsen and Stouthamer 2001; De Moor et al. 2008; Hofstede et al. 1989). For a more comprehensive overview of these studies see Ward et al. (2008).

The results of hydrological modelling results for the future tend to agree that mean winter season Meuse discharge in the twenty-first century will be greater than that in the twentieth century (e.g. Booij 2005; Bultot et al. 1988, 1990; De Wit et al. 2001;

Gellens and Roulin 1998; Middelkoop et al. 2004; Van Deursen and Middelkoop 2001), as a result of higher winter precipitation totals (e.g. Booij 2005; Bultot et al. 1988, 1990; De Wit et al. 2001, 2007b; Gellens and Roulin 1998; Giorgi and Coppola 2007; Kwadijk and Rotmans 1995; Van den Hurk et al. 2006). For the summer half-year and summer season, hydrological modelling results show more inter-model and inter-scenario variation (e.g. De Wit et al. 2001; Gellens and Roulin 1998; Können 1999; Middelkoop et al. 2004). This variation can be explained to a large degree by differences between the climate scenarios and climate models used; for the summer period, climate modelling results still show a wide range of future possibilities. This uncertainty is reflected in the most recent KNMI (Royal Netherlands Meteorological Institute) scenarios for the coming century (Van den Hurk et al. 2006), which show no unequivocal picture for summer season precipitation in the Netherlands.

The majority of high-flows on the Meuse occur in the winter as a result of prolonged zonal precipitation over large parts of the basin. Climate models show good agreement on the projected changes in precipitation during the winter half-year, which means that impact assessments can provide more reliable results for the winter than for the summer. Several hydrological modelling studies suggest that the frequency or magnitude of floods on the Meuse or its tributaries will be higher in the twenty-first century than in the twentieth century (e.g. Booij 2005; Bultot et al. 1988, 1990; Gellens 1991; Gellens and Roulin 1998; Leander et al. 2008; Van Deursen and Middelkoop 2001, 2002).

Few modelling studies of the Meuse have looked specifically at the effects of changes in land use. Ashagrie et al. (2006) and Tu et al. (2005) found no evidence in the observed record to suggest that land use change during the twentieth century had a significant effect on Meuse discharge. The current study indicates that in spite of the large land use changes expected in the twenty-first century at the European level (Busch 2006; Rounsevell et al. 2006; Verburg et al. 2006), the projected land use changes in the Meuse basin in the first half of the twenty-first century are small, and as a result climate impacts dominate changes in hydrology.

5.3 Implications for water management

The discharge regime of the Meuse has undergone large changes over the course of the late Holocene, due to both natural causes (i.e. long term fluctuations in climate over the course of the late Holocene); and anthropogenic causes (i.e. large-scale deforestation of the basin, and the effects of anthropogenic climate change over the last century). As such, the 'natural' discharge regime no longer exists, even ignoring the (ongoing and projected) impacts of anthropogenic climate change. The emission scenarios used in this study for the twenty-first century lie towards the upper (A2) and lower (B1) end of the full range of SRES emission scenarios (IPCC 2000) in terms of the concentration of greenhouse gases in the atmosphere by the end of the twenty-first century, and hence represent a broad spectrum of possible futures. For the first half of the twenty-first century the differences between the two scenarios are relatively small, but by the second half of the twenty-first century the effects under scenario A2 become much more severe than those under scenario B1. At present it is not possible to say which of the future pathways is more likely to occur, as this is dependent on political, socioeconomic, and technical developments at the global scale. Nevertheless, even under the more optimistic B1 scenario the changes are large, with the changes in mean annual discharge and high-flow frequency between the twentieth and twenty-first centuries being as great as the changes that have taken place over the last 4,000 years. Moreover, the projected increases in discharge and flood frequency in the twenty-first century (compared to the twentieth century) as a result of climate change occur much more rapidly than the long term changes which have taken place since 4000 BP.

Hence, the results show that increased discharge and high-flow frequencies, to values far higher than those experienced over the last 4,000 years, may be unavoidable, even if a concerted and immediate effort were undertaken at the global scale to mitigate greenhouse gas emissions. This, and the fact that the future changes are much rapid than the long-term changes over the last 4,000 years, underscores the need for continued attention and research into adaptation strategies for water management.

Whilst large-scale deforestation in the Meuse basin has had a major effect on discharge and medium-sized high-flows over the course of the late Holocene, the effects of the land use changes projected for the first half of the twenty-first century are small. Although the B1 scenario indicates that some reforestation may occur in the twenty-first century, large-scale reforestation is not expected in the Meuse basin (WUR/MNP 2007), due to the high economic demand on land and the attention to the preservation of cultural landscapes. However, whilst the effects of twenty-first century land use change on high-flow frequencies may be small, this does not necessarily mean that the impacts of land use change on flood risk (defined as the probability of flooding multiplied by the potential flood damage; Smith 1994) are small. In other basins around the world, the effects of twenty-first century land use change on discharge and high-flow frequency may be much larger. In particular, urbanisation may have a large effect on runoff. Moreover, changes in the percentage cover of forest have been shown to have a great influence on soil erosion and the delivery of sediments to rivers in the Meuse basin (Stam 2002; Ward et al. 2009).

5.4 Limitations

Recent studies by Leander and Buishand (2007) and Leander et al. (2008) show that the estimation of extreme discharge percentiles from the results of hydrological models is highly dependent on the climate model used and the method used to correct the bias of those climate models. The climate model used in this study has a low spatial resolution and simplified atmospheric physics compared to GCMs (and RCMs), which makes it difficult to precisely simulate the regional details and variability of daily precipitation. Furthermore, the downscaling of precipitation is carried out using a simple linear correction technique. Nevertheless, the discharge results are in general agreement with qualitative assessments of palaeodischarge derived from multi-proxy records of the late Holocene. Hence, the model is useful for assessing the main trends and changes over long time-scales, although the absolute values should be treated with caution.

The land use data represent only a generalised pattern of land use change over the last millennium, and do not include information on factors such as land use intensity (e.g. changes in crop types, irrigation etc.) or changes in water management measures (e.g. water retention basins; dams and weirs; canalisation). The examination of such measures would require the use of a higher resolution and a more complex hydrological model. However, the use of such a model would prohibit the examination of future changes with respect to long-term millennial changes (due to prohibitive computational time), which is the main aim of this study.

6 Conclusions

The discharge regime of the Meuse has undergone huge changes over the course of the late Holocene, due to both natural and anthropogenic causes. As such, the 'natural' discharge regime no longer exists, even ignoring the (ongoing and projected) impacts of anthropogenic climate change. Over the course of the late Holocene, both the mean discharge of the Meuse, as well as the frequency of high-flows similar in magnitude to those experienced during the major floods of 1926 and 1993, have increased. The difference between the periods 4000–3000 BP and 1000–2000 AD is mostly the result of lower mean annual evapotranspiration in the latter period due to the conversion of forest to agricultural land. However, the higher discharge and frequency of such high-flow events in the twentieth century compared to the nineteenth century are mainly due to higher (winter half-year) precipitation totals; on this timescale climate overwhelms land use change as the most important forcing mechanism. In the twenty-first century, projected anthropogenic climate change results in even greater discharge and high-flow frequency than in the twentieth century. The magnitude of extreme floods with a return period of 1,250 years is higher for the twenty-first century than for the twentieth century. Land use change has had little effect on such extreme floods, even on the millennial timescale.

One of the main values of the approach used in this study is that it allows us to delineate the effects of changes in climate and land use on long (centennial to millennial) timescales, and thereby identify mechanisms important to changes in discharge and high-flow frequency. The approach also allows us to examine the effects of anthropogenic activities against a natural reference period, which is not possible when only examining discharge records of the last century and the coming century. Furthermore, the results of the model are verified against geological and geomorphological evidence from periods in which environmental conditions were different to those of the present day. The modelling approach applied here can provide a useful tool for assessing the effects of future environmental change relative to longer-term changes in discharge and high-flow frequency in other basins around the world.

Acknowledgements This research project was carried out in the framework of the Dutch National Research Programme 'Climate changes Spatial Planning' (www.klimaatvoorruimte.nl). We would like to thank Jef Vandenberghe, Ronald van Balen (VU University Amsterdam), and Marcel de Wit (deceased 7 September 2009) for useful discussions and comments on an earlier version of the manuscript. We also thank two anonymous reviewers and the editor Stephen Schneider for their useful and constructive comments.

References

Aerts JCJH, Bouwer LM (2002) STREAM Krishna. A hydrological model for the Krishna River in India. RIKZ/Coastal Zone Management Centre, The Hague. www.geo.vu.nl/users/ivmstream/public/aerts&bouwer2002a.pdf

Aerts JCJH, Kriek M, Schepel M (1999) STREAM (Spatial tools for river basins and environment and analysis of management options): set up and requirements. Phys Chem Earth Part B Hydrol Oceans Atmos 24:591–595

Aerts JCJH, Renssen H, Ward PJ, De Moel H, Odada E, Bouwer LM, Goosse H (2006) Sensitivity of global river discharges under Holocene and future climate conditions. Geophys Res Lett 33:L19401. doi:10.1029/2006GL027493

Andréassian V (2004) Waters and forests: from historical controversy to scientific debate. J Hydrol 291:1–27. doi:10.1016/j.jhydrol.2003.1012.1015

Arnell N, Liu C, Compagnucci R, Da Cunha L, Hanaki K, Howe C, Mailu G, Shiklomanov I, Stakhiv E (2001) Hydrology and water resources. In: Houghton JT, Ding Y, Griggs DJ, Noguer M, Van der Linden PJ, Dai X, Maskell K, Johnson CA (eds) Climate change 2001: impacts, adaptation and vulnerability. Contribution of working group II to the third assessment report of the intergovernmental panel on climate change. Cambridge University Press, Cambridge, pp 193–233

Ashagrie AG, De Laat PJM, De Wit MJM, Tu M, Uhlenbrook S (2006) Detecting the influence of land use changes on discharges and floods in the Meuse River Basin—the predictive power of a ninety-year rainfall-runoff relation? Hydrol Earth Syst Sci 10:691–701

Berendsen HJA, Stouthamer E (2001) Palaeogeographic development of the Rhine–Meuse delta, the Netherlands. Koninklijke van Gorcum, Assen

Berger HEJ (1992) Flow forecasting for the River Meuse. Ph D thesis, Technische Universiteit Delft

Bohncke SJP, Vandenberghe J, Coope R, Reiling R (1987) Geomorphology and palaeoecology of the Mark valley (southern Netherlands): palaeoecology, palaeohydrology and climate during the Weichselian Late Glacial. Boreas 16:69–85. doi:10.1111/j.1502-3885.1987.tb00756.x

Bohncke SJP, Vandenberghe J (1991) Palaeohydrological development in the Southern Netherlands during the last 15000 years. In: Starkel L, Gregory KJ, Thornes JB (eds) Temperate palaeohydrology. Wiley, Chichester, pp 253–281

Booij MJ (2002) Appropriate modelling of climate change impacts on river flooding. Ph D Thesis, University of Twente, the Netherlands

Booij MJ (2005) Impact of climate change on river flooding assessed with different spatial model resolutions. J Hydrol 303:176–198. doi:110.1016/j.jhydrol.2004.1007.1013

Bouwer LM, Aerts JCJH, Van de Coterlet GM, Van de Giesen N, Gieske A, Mannaerts C (2004) Evaluating downscaling methods for preparing Global Circulation Model (GCM) data for hydrological impact modelling. In: Aerts JCJH, Droogers P (eds) Climate change in contrasting river basins. adaptation strategies for water, food and environment. CABI, Wallingford, pp 25–47

Brovkin V, Bendtsen J, Claussen M, Ganopolski A, Kubatzki C, Petoukhov V, Andreev A (2002) Carbon cycle, vegetation, and climate dynamics in the Holocene: experiments with the CLIMBER-2 model. Glob Biogeochem Cycles 16:1139. doi:1110.1029/2001GB001662,002002

Brown AE, Zhang L, McMahon TA, Western AW, Vertessy R (2005) A review of paired catchment studies for determining changes in water yield resulting from alterations in vegetation. J Hydrol 310:28–61. doi:10.1016/j.jhydrol.2004.1012.1010

Bultot F, Coppens A, Dupriez GL, Gellens D, Meulenberghs F (1988) Repercussions of a CO2 doubling on the water cycle and on the water balance—a case study for Belgium. J Hydrol 99:319–347

Bultot F, Dupriez GL, Gellens G (1990) Simulation of land use changes and impacts on the water balance—case study for Belgium. J Hydrol 114:327–348

Bunnik FPM (1995) Pollenanalytische Ergebnisse zur Vegetations- und Land-wirtschaftsgeschichte der Jülicher Lößbörde von der Bronzezeit bis in die frühe Neuzeit. Bonn Jahrb 195:313–349

Busch G (2006) Future European agricultural landscapes—what can we learn from existing quantitative land use scenario studies? Agric Ecosyst Environ 114:121–140. doi:10.1016/j.agee.2005.11.007

Claussen M, Mysak LA, Weaver AJ, Crucifix M, Fichefet T, Loutre M-F, Weber SL, Alcamo J, Alexeev VA, Berger A, Calov R, Ganopolski A, Goosse H, Lohmann G, Lunkeit F, Mokhov II, Petoukhov V, Stone P, Wang Z (2002) Earth system models of intermediate complexity: closing the gap in the spectrum of climate system models. Clim Dyn 18:579–586. doi:10.1007/s00382-001-0200-1

Cosandey C, Andréassian V, Martin C, Didon-Lescot JF, Lavabre J, Folton N, Mathys N, Richard D (2005) The hydrological impact of the Mediterranean forest: a review of French research. J Hydrol 301:235–249

De Moor JJW, Kasse C, Van Balen RT, Vandenberghe J, Wallinga J (2008) Human and climate impact on catchment development during the Holocene–Geul River, the Netherlands. Geomorphology 98:316–339. doi:10.1016/j.geomorph.2006.12.033

De Wit M, Warmerdam P, Torfs P, Uijlenhout R, Roulin E, Cheymol A, Van Deursen W, Van Walsum P, Ververs M, Kwadijk J, Buiteveld H (2001) Effect of climate change on the hydrology of the river Meuse. Dutch national research programme on global air pollution and climate change report number 410.200.090. RIVM, Bilthoven

De Wit MJM, Peeters H, Gastaud PH, Dewil P, Maeghe K, Baumgart J (2007a) Floods in the Meuse basin: event descriptions and an international view on ongoing measures. Int J River Basin Manage 5:279–292

De Wit MJM, Van den Hurk B, Warmerdam PMM, Torfs PJJF, Roulin E, Van Deursen WPA (2007b) Impact of climate change on low-flows in the river Meuse. Clim Change 82:1573–1480. doi:1510.1007/s10584-10006-19195-10582

Diermanse FLM (2004)HR2006 herberekening werklijn Maas. Report Q4623. WL Delft Hydraulics, Delft

EEA (2001) Sustainable water use in Europe. Part 3: extreme hydrological events: floods and droughts. Environmental issue report number 21. EEA, Copenhagen

Gellens D (1991) Impact of a CO_2-induced climatic change on river flow variability in three rivers in Belgium. Earth Surf Process Landf 16:619–625

Gellens D, Roulin E (1998) Streamflow response of Belgian catchments to IPCC climate change scenarios. J Hydrol 210:242–258

Gentry AH, Parody JL (1980) Deforestation and increased flooding of the Upper Amazon. Science 210:1354–1356

Giorgi F, Coppola E (2007) European climate-change oscillation (ECO). Geophys Res Lett 34:L21703. doi:21710.21029/22007GL031223

Goosse H, Fichefet T (1999) Importance of ice–ocean interactions for the global ocean circulation: a model study. J Geophys Res Oceans 104:23337–23355

Goosse H, Renssen H, Timmermann A, Bradley RS (2005) Internal and forced climate variability during the last millennium: a model-data comparison using ensemble simulations. Quat Sci Rev 24:1345–1360

Goosse H, Arzel O, Luterbacher J, Mann ME, Renssen H, Riedwyl N, Timmermann A, Xoplaki E, Wanner H (2006) The origin of the European "medieval warm period." Climate of the Past 2:99–113. www.clim-past.net/2/99/2006/

Gotjé W, Van Wayjen MCA, Van Geel B (1990) A palynological study of a Holocene deposit from Grand-Bongard (Hautes-Fagnes, Belgium). Geol Mijnb 69:227–241

Goudie A (1992) Environmental change: contemporary problems in geography. Clarendon, Oxford

Hofstede JLA, Berendsen HJA, Janssen CR (1989) Holocene palaeogeography and palaeoecology of the fluvial area near Maurik (Neder-Betuwe, the Netherlands). Geol Mijnb 68:409–419

IPCC (2000) Special report on emission scenarios. Cambridge University Press, New York

Jones JA (2000) Hydrologic processes and peak discharge response to forest removal, regrowth, and roads in 10 small experimental basins, western Cascades, Oregon. Water Resour Res 36:2621–2642

Können GP (1999) De toekomst van het Nederlandse klimaat. KNMI, De Bilt

Kundzewicz ZW, Mata LJ, Arnell NW, Döll P, Kabat P, Jiménez B, Miller KA, Oki T, Sen Z, Shiklomanov IA (2007) Freshwater resources and their management. In: Parry ML, Canziani OF, Palutikof JP, Van der Linden PJ, Hanson CE (eds) Climate Change 2007: impacts, adaptation and vulnerability. Contribution of the working group II to the fourth assessment report of the intergovernmental panel on climate change. Cambridge University Press, Cambridge, pp 173–210

Kwadijk JCJ (1993) The impact of climate change on the discharge of the River Rhine. Ph D thesis, Universiteit Utrecht

Kwadijk J, Rotmans J (1995) The impact of climate change on the River Rhine: a scenario study. Clim Change 30:397–425

Leander R, Buishand TA (2007) Resampling of regional climate model output for the simulation of extreme river flows. J Hydrol 332:487–496. doi:10.1016/j.jhydrol.2006.08.006

Leander R, Buishand TA, Van den Hurk BJJM, De Wit MJM (2008) Estimated changes in flood quantiles of the river Meuse from resampling of regional climate model output. J Hydrol 351:331–343. doi:10.1016/j.jhydrol.2007.12.020

Mahe G, Paturel J-E, Servat E, Conway D, Dezetter A (2005) The impact of land use change on soil water holding capacity and river flow modelling in the Nakambe River, Burkina-Faso. J Hydrol 300:33–43

Middelkoop H, Van Asselt MBA, Van 't Klooster SA, Van Deursen WPA, Kwadijk JCJ, Buiteveld H (2004) Perspectives on flood management in the Rhine and Meuse Rivers. River Res Appl 20:327–342

Mitchell TD, Jones PD (2005) An improved method of constructing a database of monthly climate observations and associated high-resolution grids. Int J Climatol 25:693–712. doi:10.1002/joc.1181

Opsteegh JD, Haarsma RJ, Selten FM, Kattenberg A (1998) ECBILT: a dynamic alternative to mixed boundary conditions in ocean models. Tellus 50A:348–367

Renssen H, Goosse H, Fichefet T, Brovkin V, Driesschaert E, Wolk F (2005) Simulating the Holocene climate evolution at northern high latitudes using a coupled atmosphere–sea–ice–ocean–vegetation model. Clim Dyn 24:23–43

Rounsevell MDA, Reginster I, Araújo MB, Carter TR, Dendoncker N, Ewert F, House JI, Kankaanpää S, Leemans R, Metzger MJ, Schmit C, Smith P, Tuck G (2006) A coherent set of land use change scenarios for Europe. Agric Ecosyst Environ 114:57–68. doi:10.1016/j.agee.2005.11.027

RWS Limburg/IWACO (2000) Internationale ecologische verkenning Maas (EVIM). Historisch ecologische oriëntatie op het stroomgebied (fase 2a). Rijkswaterstaat Directie Limburg, Afdeling Integraal Waterbeleid, Maastricht

Smith DI (1994) Flood damage estimation—a review of urban stage-damage curves and loss functions. Water SA 20:231–238

Stam MH (2002) Effects of land-use and precipitation changes on floodplain sedimentation in the nineteenth and twentieth centuries (Geul River, the Netherlands). In: Martini IP, Baker VR, Garzón G (eds) Flood and megaflood processes and deposits: recent and ancient examples. Blackwell Science, Oxford, pp 251–267

Thornthwaite CW (1948) An approach toward a rational classification of climate. Geogr Rev 38:55–94

Thornthwaite CW, Mather JR (1957) Instructions and tables for computing potential evapotranspiration and the water balance. Publ Climatol 10:183–243

Tu M, Hall MJ, De Laat PJM, De Wit MJM (2005) Extreme floods in the Meuse river over the past century: aggravated by land-use changes? Phys Chem Earth, Parts A/B/C 30:267–276

Van den Hurk B, Klein Tank A, Lenderink G, Van Ulden A, Van Oldenborgh GJ, Katsman C, Van den Brink H, Keller F, Bessembinder J, Burgers G, Komen G, Hazeleger W, Drijfhout S (2006) KNMI Climate change scenarios 2006 for the Netherlands. KNMI Scientific Report WR 2006-01. KNMI, De Bilt

Van Deursen WPA, Middelkoop H (2001) Development of flood management strategies for the Rhine and Meuse basins in the context of integrated river management. Executive summary of the IRMA-SPONGE Project 3/NL/1/164/99 15 183 01. Netherlands Centre for River Studies, Rotterdam

Van Deursen WPA, Middelkoop H (2002) Development of flood management strategies for the Rhine and Meuse basins in the context of integrated river management. Executive summary of the IRMA-SPONGE Project 2. In: Hooijer A, Van Os A (eds) Towards sustainable flood risk management in the Rhine and Meuse River basins. NCR, Delft

Van Geel B, Buurman J, Waterbolk HT (1996) Archaeological and palaeoecological indications of an abrupt climate change in The Netherlands, and evidence for climatological teleconnections around 2650 BP. J Quat Sci 11:451–460. doi:10.1002/(SICI)1099-1417(199611/12)11:6<451::AID-JQS275>3.0.CO;2-9

Van Rompaey AJJ, Govers G, Puttemans C (2002) Modelling land use changes and their impact on soil erosion and sediment supply to rivers. Earth Surf Process Landf 27:481–494. doi:410.1002/esp.1335

Verburg PH (2006) Simulating feedbacks in land use and land cover models. Landsc Ecol 21:1171–1183. doi:1110.1007/s10980-10006-10029-10984

Verburg PH, Schulp CJE, Witte N, Veldkamp A (2006) Downscaling of land use change scenarios to assess the dynamics of European landscapes. Agric Ecosyst Environ 114:39–56

Verburg PH, Eickhout B, Van Meijl H (2008) A multi-scale, multi-model approach for analyzing the future dynamics of European land use. Ann Reg Sci 42:57–77. doi:10.1007/s00168-00007-00136-00164

Ward PJ, Aerts JCJH, De Moel H, Renssen H (2007) Verification of a coupled climate–hydrological model against Holocene palaeohydrological records. Glob Planet Change 57:283–300. doi:10.1016/j.gloplacha.2006.12.002

Ward PJ, Renssen H, Aerts JCJH, Van Balen RT, Vandenberghe J (2008) Strong increases in flood frequency and discharge of the River Meuse over the late Holocene: impacts of long-term anthropogenic land use change and climate variability. Hydrol Earth Syst Sci 12:159–175. www.hydrol-earth-syst-sci.net/112/159/2008.

Ward PJ, Van Balen RT, Verstraeten G, Renssen H, Vandenberghe J (2009) The impact of land use and climate change on late Holocene and future suspended sediment yield of the Meuse catchment. Geomorphology 103:389–400. doi:10.1016/j.geomorph.2008.07.006

Westhoek HJ, Van den Berg M, Bakkes JA (2006) Scenario development to explore the future of Europe's rural areas. Agric Ecosyst Environ 114:7–20. doi:10.1016/j.agee.2005.1011.1005

WUR/MNP (2007) Eururalis 2.0 CD-ROM. Wageningen UR, Wageningen

Zagwijn WH (1994) Reconstruction of climate change during the Holocene in western and central Europe based on pollen records of indicator species. Veg Hist Archaeobot 3:65–88. doi:10.1007/BF00189928